Dynamics of Glasslike Transitions in a Quasi-Two-Dimensional System

Y. H. Hwang and X-l. Wu

Department of Physics and Astronomy, University of Pittsburgh, Pittsburgh, Pennsylvania 15260

(Received 25 May 1994; revised manuscript received 8 December 1994)

Transverse self-diffusion of field-induced magnetic colloidal chains is measured using real-space imaging. It has been found that the mean-square displacement $\langle \Delta r^2 \rangle$ depends on the aligning field H and displays two different behaviors. In short times $\langle \Delta r^2 \rangle$ is subdiffusive, whereas in long times $\langle \Delta r^2 \rangle$ exhibits normal diffusion. The characteristic time separating the two time regimes diverges exponentially with H, indicating fast frozen-in density fluctuations in the system. Our experimental results deviate significantly from the predictions of mode-coupling theory.

PACS numbers: 64.70.Pf, 51.20.+d, 61.50.–f, 63.20.–e

In this Letter we present an experimental study of transverse self-diffusion of magnetic chains in the presence of an aligning magnetic field H. The unique features of the experiment are that the motion of the chains is sufficiently slow, allowing video imaging of "microscopic" dynamics, and that the interactions between the chains are continuously tunable, allowing exploration of scaling behaviors over extended time scales. It was found that in short times the array of magnetic chains behaves like a solid, whereas in long times it behaves like a liquid. The characteristic time t^* separating the two regimes is of the order of a second in weak fields and increases exponentially with H. It appears that the conventional hexatic phase, expected in a two-dimensional 2D system, is preempted by a glass transition, and the system possesses no long-range positional and orientational orders in the strong-field limit.

Being imbedded in a quasi-2D space, the structure of an array of magnetic chains is susceptible to small disturbances. Thermal fluctuations, pinning due to walls, and randomness in the coupling constant between the chains all conspire to make the lattice disordered. In this regard, our system is somewhat similar to that of the Abrikosov lattice in type-II superconductors, which has attracted a great deal of attention [1]. An intriguing issue which is at the heart of all this research is the effect of the disorders on the dynamics of line objects [2]. An understanding of how these line objects move is not only academically challenging but also practically useful in producing robust superconductors and controlling defect motions in liquid crystals.

The system under investigation is an aqueous suspension of magnetic particles of 0.8 μm in diameter and 2% in concentration [3]. The sample was confined between two parallel sapphire plates separated by 12.5 μm and placed in a long solenoid with H normal to the plates. In the H field individual particles acquire a magnetic dipole moment $\boldsymbol{\mu} \sim \mathbf{H}$. If H is strong enough, the particle-particle interaction overwhelms the thermal energy, causing them to assemble into an array of chains parallel to the field. For this system, the onset of chain formation occurs at ~6 Oe. Once formed the diameter of the chains is approximately equal to a particle diameter and has polydispersity of ~20%, as viewed under a microscope. The chains interact via a repulsive dipole-dipole interaction, which can be tuned continuously by varying H. Using small-angle light scattering and video imaging [4], it was found that the spatial arrangement of the chains depends on both H and $\dot{H}$, the ramping rate of the field. By varying H abruptly the lattice is disordered, whereas by varying H sufficiently slowly, $\dot{H} \sim 1$ Oe/h, a fairly regular lattice can be formed. In the current experiment we used this slow ramping rate, and H was held constant during measurements.

The end positions of the magnetic chains were imaged using an optical microscope (500×) and recorded in real time (1 image/s) using a computer. The area studied (70×100 μm^2) is very small compared to the size of the sample which is ~1 cm^2. A particle tracing software allows us to follow the motion of ~100 chains simultaneously and to determine their positions with an accuracy of ± 1 pixel (~0.3 μm).

Figures 1(a) and 1(b) show two configurations of the magnetic chains for $H = 8$ and 25 Oe, respectively, As can be seen, despite a weak field dependence of both the radius and the density of the chains, the structure of the array changes remarkably as H increases. For low fields, the end positions of the chains are almost uncorrelated, corresponding to a liquid. For high fields, on the other hand, the local crystallographic axes are clearly identifiable. For $H > 30$ Oe, the system is frozen with no structural rearrangement upon further increase of H. In this frozen state, the system possesses no long-range positional and orientational orders, as indicated by the exponential decay of the corresponding correlation functions and short correlation lengths, which are of the order of a lattice spacing a.

From a sequence of pictures taken at a fixed H, we calculated the probability density function (PDF) $P(x, t)$. Physically, $P(x, t)$ is the conditional probability of finding a chain at a position x at time t, when the chain is at $x = 0$ for $t = 0$. Here since the system is translationally invariant in both space and time, the origins of x and t

 0031-9007/95/74(12)/2284(4)$06.00 © 1995 The American Physical Society

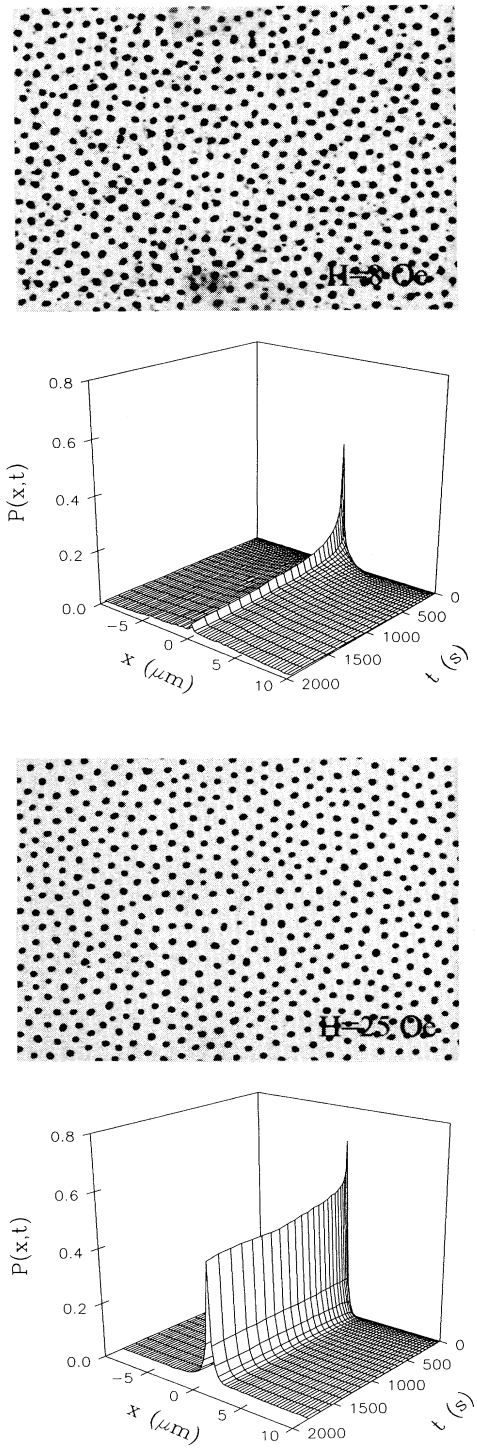

FIG. 1. Structure and dynamics of magnetic chains. The measurements are for magnetic fields (a) $H = 8$ and (b) 25 Oe. The chains become more ordered as H increases. Correspondingly, the probability density $P(x,t)$ decays rapidly in time t for the low field, whereas $P(x,t)$ decays slowly for the high field.

are arbitrary. We found that in order to have reliable measurement of the PDF the time average alone is not adequate. This is particularly the case for high fields, where individual chains only explore a limited configurational space, giving rise to nonergodic behavior. To overcome irregularities in the data, an ensemble of measurements were carried out, and $P(x,t)$ was obtained using both the time and the ensemble averages. The PDF at $H = 8$ and 25 Oe are shown underneath the pictures in Fig. 1. For the low field, $P(x,t)$ is approximately a Gaussian in x and its amplitude decreases as $t^{-1/2}$. In comparison, for the high field, $P(x,t)$ is strongly non-Gaussian and its amplitude decays by less than 40% over several thousand seconds. The motion of the chains, hence the density fluctuations, is essentially frozen at long times.

For an isotropic system, the PDF along the x direction should be the same as along the y direction, $P(x,t) = P(y,t)$. This is indeed the case in our measurements. The measured PDF allows for the calculation of the mean-square displacement (MSD) $\langle \Delta r^2(t) \rangle$ of a tracer chain. Figure 2(a) shows a set of MSD measurements for $8 \leq H \leq 30$ Oe. Within this range of H, the MSD at long

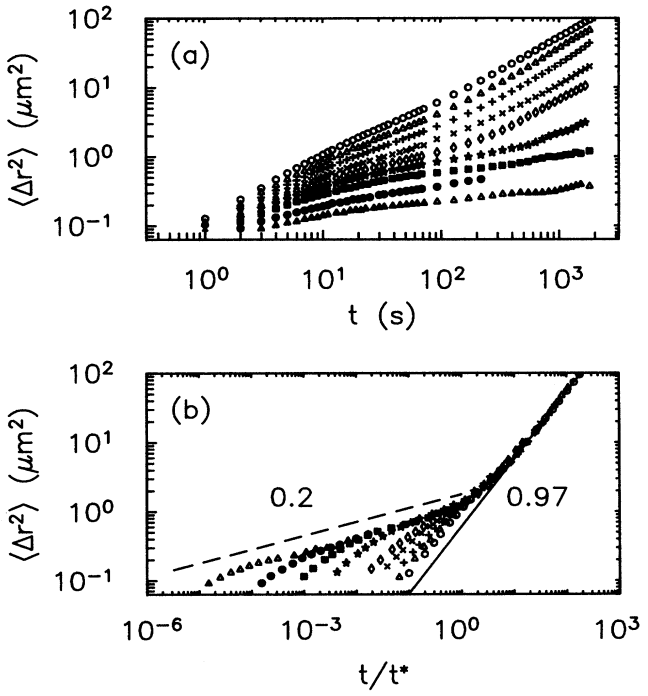

FIG. 2. The MSD vs time. (a) The measurements were performed at $H = 8$ (open circles), 10 (open triangles), 12 (plusses), 14 (crosses), 16 (open diamonds), 18 (stars), 20 (solid squares), 25 (solid circles), and 3 (solid triangles). (b) The scaling plot of MSD vs t/t^*. By rescaling the t axis the long-time diffusion can be collapsed onto a single curve with a slope of 0.97. The intermediate-time regime also scales with a common slope of ~0.2.

times changes by nearly 3 orders of magnitude. For $H \leq 18$ Oe, all the curves show a characteristic S shape; the MSD increases rapidly in short times, then slows down in intermediate times, and finally increases again at long times. In the short-time regime, the initial slope of the MSD decreases with H. If a power-law $\langle \Delta r^2 \rangle \sim t^{\alpha}$ is assumed, which has only limited range, the exponent α is found to be ~ 1 for weak fields, and it levels off at ~ 0.2 as H approaches 30 Oe. The short-time diffusion, therefore, changes smoothly from normal diffusion to subdiffusion. The slowing down of transverse diffusion in the intermediate times, forming a plateau in the MSD, appears to be ubiquitous and its range increases markedly with the field. For $H > 18$ Oe, the MSD is completely dominated by the plateau regime even for times as long as 2000 s. However, based on the trend seen for the low fields, it is reasonable to extrapolate that the long-time diffusion behavior may still persist, manifesting itself at a time scale that is not reached by the current measurements.

The similarity in the MSD at long times motivates a scaling plot of $\langle \Delta r^2(t) \rangle$ vs a reduced time t/t^*, where the characteristic time t^* is a function of H. On the log-log plot this scaling procedure is equivalent to a horizontal shift of the individual curves in Fig. 2(a) by an amount such that the MSD at long times collapses onto a single curve. As shown in Fig. 2(b), over two decades in t/t^*, an excellent collapse of the data is obtained, and the master curve has a slope of 0.97 ± 0.03 as delineated by the solid line in the figure. The slope is close to unity, suggesting that the self-diffusion on large times or length scales is uncorrelated. It is interesting that the above scaling procedure reveals an additional power-law behavior for the intermediate times [5]. For $10^{-5} \leq t/t^* < 10^{0}$, all the data seem to follow the same trend with a common slope of ~ 0.2, as shown by the dashed line. We noted that the crossover from the intermediate to the long-time behaviors appears to be sharp on this scaling plot with a crossover length $\sqrt{\langle \Delta r_C^2 \rangle} \sim 1$ μm. Since the average spacing between the chains is $a \simeq 7$ μm, we found that $\sqrt{\langle \Delta r_C^2 \rangle}/a^2 \simeq 14\%$, which coincides remarkably well with the Lindemann's melting criterion for 3D solids. The result is somewhat surprising since one expects that thermal fluctuations for our quasi-2D system should be more significant than in 3D; hence a tighter bound is anticipated.

Physically, t^* can be identified as the escape time of a typical chain from its local potential energy minimum. The t^* was found to increase exponentially with H, and the behavior can be described by an Arrhenius law, $t^* = t_0 \exp(\Delta E/k_B T)$, where ΔE is the typical energy barrier. Because of long-range dipole-dipole interactions, the relevant energy scale is $\Delta E \sim v^2 \chi^2 H^2/a^3$, where v and χ are the volume and the magnetic susceptibility of the chain. The time t_0 may be thought of as the collision time of the chain with the energy barrier, and the relevant time scale is d^2/D_0, where d and D_0 are the diameter and the free diffusion constant of the chain. The relation $t^* = t_0 \exp(cH^2)$ is well borne out by the plot (solid circles) in Fig. 3. It was found that $c(\equiv \Delta E/k_B T H^2) \simeq 0.012$ Oe^{-2} and $t_0 \simeq 6$ s; both agree well with the theoretical estimates taking $\chi = 0.07$ and $D_0 = 10^{-9}$ cm^2/s which are measured independently. The exponential increase in t^* prevents the system from seeking the potential energy minimum effectively, causing it to be trapped in a metastable, disordered glassy state in high fields [4].

We have also calculated the long-time self-diffusion coefficient D by analyzing the MSD data for $t > t^*$. As shown in the inset of Fig. 3, D decreases by nearly 2 orders of magnitude as H increases from 8 to 18 Oe. Quantitatively, $D(H)$ can also be described by an Arrhenius law $D(H) = D_0 \exp(-\Delta E/k_B T) = D_0 \exp(-cH^2)$, and the parameters D_0 and c turn out to be nearly identical to those used for describing t^*. Thus we have achieved a fit to $D(H)$ with no adjustable parameters, as shown by the solid line in the inset. The simple equation describing the field dependence of both t^* and D is reassuring, and suggests that the dynamics of the system is governed by only a few parameters.

What is the physical mechanism that produces the subdiffusive behavior in short and intermediate times? Neglecting disorder, the phenomenon may be modeled as thermal motion of a lattice "atom" which is coupled to long wavelength collective modes. The problem can be solved in a systematic fashion using a Langevin equation. In two dimensions it can be shown that the MSD diverges logarithmically in time $\langle \Delta r^2(t) \rangle \sim \ln(t)$,

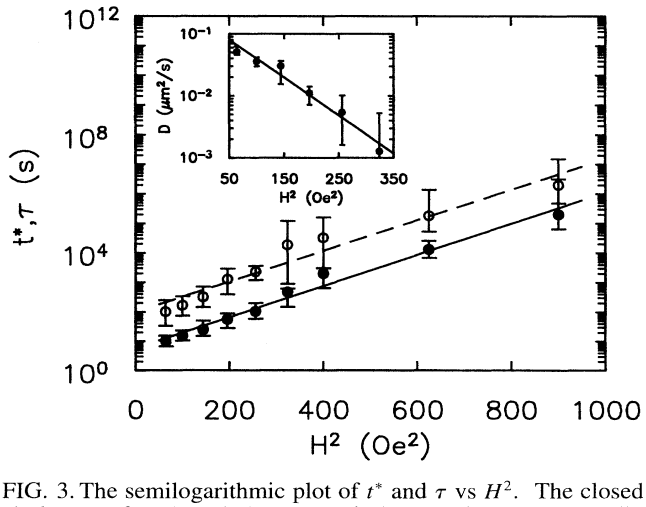

FIG. 3. The semilogarithmic plot of t^* and τ vs H^2. The closed circles are for t^* and the open circles are for τ. The solid and the dashed lines are fits to the Arrhenius law. The inset shows the semilogarithmic plot of the long-time self-diffusion coefficient D vs H^2.

implying the absence of long-range translational order in 2D. The predicted logarithmic time dependence, however, is inconsistent with our observations and suggests that disorder in the lattice structure and thermally activated cluster motions may also be important.

The short translational and orientational correlation lengths and fast frozen-in density fluctuations are strongly suggestive that our system undergoes a glass transition as H increases. We have made an attempt to compare our observations with the mode-coupling theory (MCT) [6], which makes detailed predictions for the dynamics near a glass transition. The hallmark of the MCT is the prediction of two characteristic decays, the α and the β processes. The α decay is associated with the long-time relaxation, signaling the breakdown of particle cages and the onset of long-distance diffusion of a tracer particle. On the other hand, the β decay is associated with short and intermediate time scales, reflecting a relatively slow local motion of the particle. Our observed transverse self-diffusion of magnetic chains falls naturally into the above classification of the two relaxation processes.

Within the MCT it was further shown that the self-part of the intermediate scattering function (SISF) $F^s(q,t) \sim \langle \sum_i \exp[i\mathbf{q} \cdot (\mathbf{r}_i(t) - \mathbf{r}_i(0))] \rangle$ decays in two steps, in accordance with the aforementioned α and β processes. The crossover from the β to the α relaxation forms a plateau whose width increases markedly as the glass transition is approached from the liquid side. In light of this, we have constructed the SISF by taking Fourier transformations of the measured PDF. For convenience, the wave number was set to $q = 2\pi/a$, which corresponds to the first peak in the static structure factor. Figure 4 shows nine different runs for $8 \leq H \leq 30$ Oe. Unlike the MSD data, the SISF does not exhibit sharp features that can be identified as crossovers from the short-time to the long-time dynamics. The SISF can be approximately fit to a stretched-exponential function $F^s(q,t) = \exp[-(t/\tau)^\gamma]$ with $\gamma = 0.5 \pm 0.1$ for all different runs. The relaxation time τ, on the other hand, depends critically on H and shows a similar H dependence as t^*, as indicated by the open circles in Fig. 3. Here τ is about a factor of 10 greater than t^*, which may be expected since τ is the diffusion time on the scale of a determined by the inverse of the wave number q, whereas t^* is the diffusion time on the scale of a fraction of a determined by the Lindemann's criterion.

In conclusion, the dynamics of a glass transition in a quasi-2D system has been studied from a different, yet complementary, point of view, in comparison with the more traditional scattering techniques [7,8]. The self-diffusion measurements show clearly the existence of the caging effect, resulting from the long-range interactions of the magnetic chains. However, the observed caging effect does not cause a two-step relaxation in the SISF as commonly seen for 3D glassy systems [7]. A plausible explanation for the absence of the plateau regions in the SISF may be a result of thermal activation, which plays a significant role in this quasi-2D system.

We would like to thank W. I. Goldburg, D. Jasnow, H. Kellay, and B. Martin for helpful discussions. This research is supported by the American Chemical Society under Grant No. PRF 26567-AC9.

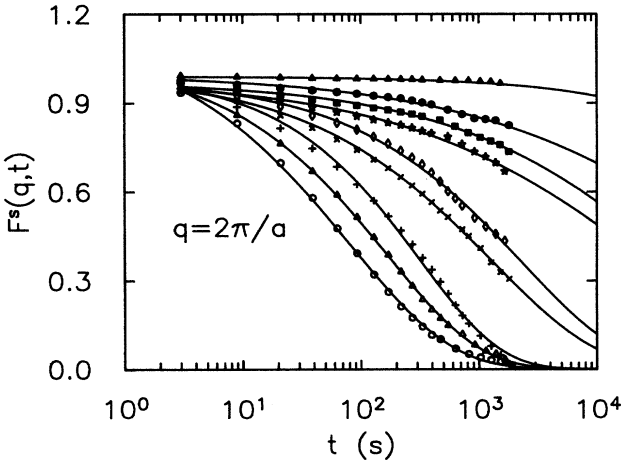

FIG. 4. The SISF $F^s(q,t)$ vs time t. The use of the symbols are the same as in Fig. 2(a) for different H. Typical uncertainties in the SISF are about 20%. The solid lines are fits to a stretched exponential function $F^s(q,t) = \exp[-(t/\tau)^\gamma]$, with $\gamma \sim 0.5$.

[1] M. P. A. Fisher, Phys. Rev. Lett. **62**, 1415 (1989); D. S. Fisher, M. P. A. Fisher, and D. A. Huse, Phys. Rev. B **43**, 130 (1991).

[2] C. Tang, S. Feng, and L. Golubovic, Phys. Rev. Lett. **72**, 1264 (1994).

[3] The particles were purchased from Bangs Laboratories, Carmel, IN 46032.

[4] Y. H. Hwang and X.-l. Wu, Phys. Rev. E **49**, 3102 (1994).

[5] For $H > 18$ Oe, though there is about a decade in which the MSD overlap with each other in the plateau regime, the uncertainty in determining t^* is still large. In the worst scenario, $H = 30$ Oe, the uncertainty in t/t^* is about 5, as indicated by the large error bars in Fig. 3.

[6] E. Leutheusser, Phys. Rev. A **29**, 2765 (1984); W. Gotze, in *Liquids, Freezing and the Glass Transition,* Proceedings of the Les Houches Summer School, Session LI edited by D. Lesvesque, J. P. Hansen, and J. Zinn-Justin (North-Holland, Amsterdam, 1991).

[7] W. van Megen and P. N. Pusey, Phys. Rev. A **43**, 5429 (1991); D. Sidebottom, R. Bergman, L. Borjesson, and L. M. Torell, Phys. Rev. Lett. **71**, 2260 (1993).

[8] J. Wuttke, J. Hernandez, G. Li, G. Coddens, H. Z. Cummins, F. Fujara, W. Petry, and H. Sillescu, Phys. Rev. Lett. **72**, 3052 (1994).

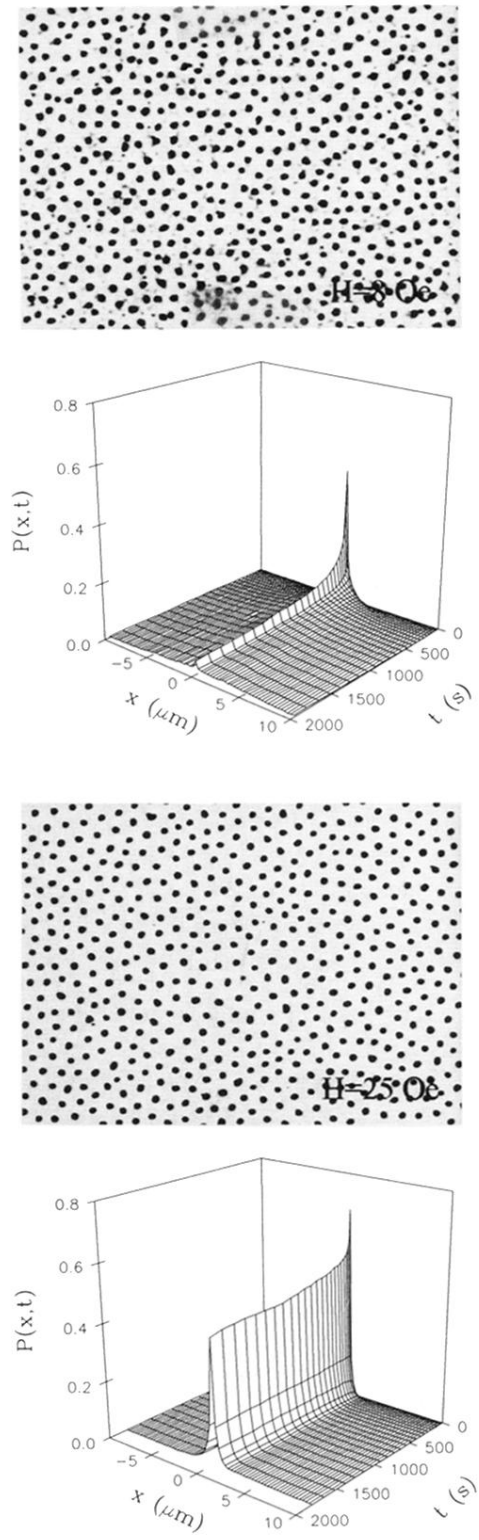

FIG. 1. Structure and dynamics of magnetic chains. The measurements are for magnetic fields (a) $H = 8$ and (b) 25 Oe. The chains become more ordered as H increases. Correspondingly, the probability density $P(x, t)$ decays rapidly in time t for the low field, whereas $P(x, t)$ decays slowly for the high field.